

Cadherins Mediate Intercellular Mechanical Signaling in Fibroblasts by Activation of Stretch-sensitive Calcium-permeable Channels*

Received for publication, May 7, 2001, and in revised form, July 19, 2001
Published, JBC Papers in Press, July 20, 2001, DOI 10.1074/jbc.M104106200

Kevin S. Ko‡, Pamela D. Arora, and Christopher A. G. McCulloch

From the Canadian Institutes of Health Research Group in Matrix Dynamics Faculty of Dentistry, University of Toronto, Toronto, Ontario M5S 3E2, Canada

Cells in mechanically active environments form extensive, cadherin-mediated intercellular junctions that are important in tissue remodeling and differentiation. Currently, it is unknown whether adherens junctions in connective tissue fibroblasts transmit mechanical signals and coordinate multicellular adaptations to physical forces. We hypothesized that cadherins mediate intercellular mechanotransduction by activating calcium-permeable, stretch-sensitive channels. Human gingival fibroblasts in suspension were plated on established homotypic monolayer cultures. The cells formed intercellular adherens junctions. Controlled mechanical forces were applied to intercellular junctions by electromagnets acting on cells containing internalized magnetite beads. At early but not later stages of intercellular attachment, force application visibly displaced magnetite bead-loaded cells and induced robust Ca^{2+} transients (65 ± 9.4 nM above base line). Similar Ca^{2+} transients were induced by force application to anti-N-cadherin antibody-coated magnetite beads. Ca^{2+} responses depended on influx of extracellular Ca^{2+} through mechanosensitive channels because both Ca^{2+} chelation and gadolinium chloride abolished the response and MnCl_2 quenched fura-2 fluorescence after force application. Force application induced accumulation of microinjected rhodamine-actin at intercellular contacts; actin assembly was inhibited by buffering intracellular calcium fluxes. Our results indicate that mechanical forces applied to adherens junctions activate stretch-sensitive calcium-permeable channels and increase actin polymerization. We suggest that N-cadherins in fibroblasts are intercellular mechanotransducers.

Intercellular junctions are dynamic structures essential for the maintenance of tissue integrity (1) and tissue repair after injury (2), for coordination of tissue remodeling responses to physiological forces (3), and for elaboration of protective adaptations as a result of pathological forces (4). In wound healing, intercellular contacts involving interactions between cadherins, actin, and myosin have been implicated in generating the forces required for wound closure (5). Notably, maintenance

of the structure of intercellular contacts critically depends upon contractile forces generated by the actin cytoskeleton (6) that act on intercellular contacts in adjacent cells (7). Collectively, these data suggest that force application to intercellular junctions is of central importance in tissue homeostasis, but the specific role of intercellular junctional proteins in transducing physical forces into regulatory signals is poorly understood.

Tension transmitted through adherens junctions can change the viscoelastic properties of fibroblasts (8) and may initiate intercellular mechanotransduction via calcium wave propagation through gap junctions (9–11). However, mechanotransduction through intercellular adherens junctions of connective tissue cells has not been examined in detail. Consequently the mechanisms of force-sensing and signal transduction at intercellular junctions remain largely unknown. Studies of biomechanical stimulation to intercellular junctions have typically used fluid flow stress or stretching of deformable substrates to apply forces to confluent cell monolayers. For example, endothelial cells exhibit profound changes in cell shape in response to altered shear stress, and these responses require reorganization of intercellular adherens junctions (12). However, it is not clear whether the morphological changes of intercellular junctions observed in these and related experiments were a direct result of force application to the junctions or were secondary to alterations in cell-substratum adhesions. Further, the nature of the signals that are generated as a result of direct mechanical stimulation of intercellular adhesions remains elusive.

To test whether intercellular adhesion complexes can transmit mechanical signals, we developed and characterized a novel model system that delivers controlled physical forces (~ 30 – 150 pN)¹ to intercellular junctions, and we measured $[\text{Ca}^{2+}]_i$ when these junctions were stretched. We used fibroblasts from periodontal connective tissues because these cells form extensive intercellular adherens and gap junctions *in vivo* (13, 14) and *in vitro* (15). Further, periodontal cells are subjected constitutively to high amplitude mechanical loads *in vivo*. With the use of specific gap junction inhibitors and anti-cadherin antibody-coated magnetic beads, we delineated the role of cadherin-mediated adherens junctions in intercellular mechanotransduction. Our major finding is that mechanical forces applied to intercellular junctions induce robust intracellular calcium transients independent of gap junctions. To the best of our knowledge, this is the first study showing that forces transmitted specifically through cadherins can activate a sec-

* This work was supported by a Canadian Institutes of Health Research Group Grant and Maintenance Grant as well as a Heart and Stroke Foundation grant (to C. A. G. M.) and a CIHR Fellowship (to K. S. K.). The costs of publication of this article were defrayed in part by the payment of page charges. This article must therefore be hereby marked "advertisement" in accordance with 18 U.S.C. Section 1734 solely to indicate this fact.

‡ To whom correspondence should be addressed: Rm. 244, Fitzgerald Bldg., University of Toronto, 150 College St., Toronto, ON M5S 3E2, Canada. Tel.: 416-978-6684; Fax: 416-978-5956; E-mail: kevin_ko@hotmail.com.

¹ The abbreviations used are: N, newton; FITC, fluorescein isothiocyanate; BAPTA/AM, [1,2-bis(*o*-amino-5-bromophenoxy)ethane-*N,N,N',N'*-tetraacetic, 4Na]; mag, mag-fura2; α -MEM, α -minimal essential medium; PBS, phosphate-buffered saline; S cells, suspended cells; A cells, substrate-attached cells; ER, endoplasmic reticulum.

ond messenger system and induce actin polymerization at force application sites.

EXPERIMENTAL PROCEDURES

Reagents—Primary antibodies against human proteins included mouse monoclonal anti- β -catenin (Clone 14), FITC-conjugated anti-CD90 (Clone 5E10), anti-pan-cadherin (Clone CH-19) (Transduction Laboratories, Lexington, KY), anti-N-cadherin (anti-A-cell adhesion molecule; Clone GC-4), anti-COX-1, and FITC-goat anti-mouse antibodies (Sigma). Rhodamine-phalloidin, cytochalasin D, thapsigargin, magnetite beads, ATP, manganese chloride, gadolinium chloride, and β -glycyrrhetic acid were purchased from Sigma. 4',6-Diamidino-2-phenylindole, HCl, Alexa Fluor 488 phalloidin, BAPTA/AM, Calcein/AM, fura-2/AM, and mag-fura-2 were purchased from Molecular Probes (Eugene, OR). Rhodamine-labeled monomeric actin was purchased from Cytoskeleton (Denver, CO). BioMag goat anti-mouse IgG (Fc specific) coated magnetic particles were purchased from Polysciences (Warrington, PA). Propidium iodide was purchased from Calbiochem (La Jolla, CA). Connexin 43 mimetic peptides including GAP 20 (amino acid sequence EIKKFKYGC) and GAP 27 (amino acid sequence SRPTEK-TIFII) were synthesized by the Alberta Peptide Institute (Edmonton, Canada).

Cell Culture—Human gingival fibroblasts were derived from primary explant cultures as described (16). The cells from passages 6–10 were grown as monolayers in T-75 flasks. Full growth medium consisted of α -minimal essential medium (α -MEM), antibiotics (0.017% penicillin G (Ayerst Laboratory, Montreal, Canada), 0.01% gentamycin sulfate (Life Technologies, Inc.), in α -MEM), and 10% (v/v) heat-inactivated fetal bovine serum (ICN Biomedicals, Costa Mesa, CA). The cells were grown to confluence prior to all experiments except when sparse cultures were used as indicated.

Immunocytochemistry—To identify and localize specific molecules involved in cell-to-cell adhesion, immunocytochemistry was performed for cadherins (using pan-cadherin antibody) and β -catenin. Cells grown on coverslips were fixed and permeabilized with methanol at -20°C for 10 min, blocked with 1:1000 mouse serum in PBS for 10 min, and incubated with primary antibody (1:100 dilution) for 1 h at room temperature, washed three times with PBS containing 0.2% bovine serum albumin, and incubated with FITC-conjugated goat anti-mouse (1:100). Nonspecific control staining was performed on a separate coverslip using an irrelevant isotype control antibody and secondary antibody.

Confocal Microscopy—Laser scanning confocal microscopy was used to locate and quantify adhesive proteins at the intercellular interface between suspended (S) and substrate-attached (A) cells as described (17). For FITC-labeled antibodies, excitation was set at 488 nm, and emission was collected with a 530/20 nm barrier filter. The cells were imaged with a 63 \times oil immersion lens (numerical aperture = 1.4), and transverse optical sections were obtained from the level of cell attachment at the substratum of the A cell to the dorsal surface of the S cell (as verified by phase contrast microscopy). The cell-to-cell interface was estimated to be located at about the middle optical section between the cells and further verified by visual assessment of the position of the nuclei of the top and bottom cells (4',6-diamidino-2-phenylindole, HCl staining).

Intracellular Calcium—For measurement of whole cell intracellular calcium ion concentration ($[\text{Ca}^{2+}]_i$), the cells on coverslips were loaded at 37°C with 3 μM fura-2/AM for 20 min. For estimation of ER calcium stores, the cells were incubated with mag-fura-2/AM (4 μM) (18) for 150 min at 37°C , in α -MEM containing fetal bovine serum (10%) (19). The calcium-free buffer is composed of 150 mM NaCl, 5 mM KCl, 10 mM D-glucose, 1 mM MgSO_4 , 1 mM Na_2HPO_4 , and 20 mM HEPES, pH 7.4, with an osmolality of 291 mOsmol. For experiments requiring external calcium, 1 mM CaCl_2 was added to the buffer. The attached cells on coverslips were washed twice and transferred to a tissue culture chamber (Corning, Corning, NY). After incubation with fura-2/AM, inspection of cells by fluorescence microscopy demonstrated no vesicular compartmentalization of fura-2, suggesting that the dye loading method allows measurement of cytosolic $[\text{Ca}^{2+}]_i$. Visual inspection of mag-fura-2-loaded cells showed fluorescent labeling of discrete intracellular organelles.

Whole cell $[\text{Ca}^{2+}]_i$ measurements were obtained with a Nikon Diaphot II inverted microscope optically interfaced to a Deltascan 4000, dual beam, epifluorescence spectrofluorimeter, and analysis system (Photon Technology Int., London, Canada). The dual excitation fluorochromes fura-2 or mag-fura-2 were excited at alternating wavelengths of 346 and 380 nm from dual monochromators with slit widths set at 2 nm. Emitted fluorescence was collected with a 40 \times quartz 1.32 numer-

ical aperture oil immersion Nikon Fluor objective and passed through a 530/20 nm barrier filter (Omega Optical, Brattleboro, VT). A variable aperture, intrabeam mask was used to restrict measurements to single cells. Estimates of $[\text{Ca}^{2+}]_i$, independent of the precise intracellular concentration of fura-2 were calculated from dual excitation emitted fluorescence according to the equation of Grynkiewicz *et al.* (20) and as described earlier (21). $[\text{Ca}^{2+}]_i$ transients of S cells and A cells were measured in separate experiments.

Internalization of Ferric Oxide Beads—Ferric oxide microparticles (Fe_3O_4 ; Aldrich) were sonicated to eliminate clumps. Particles exhibited a heterogeneous size distribution with a pronounced modal peak at $\sim 5 \mu\text{m}$. Beads were rinsed in PBS, washed three times, and resuspended in Ca^{2+} - Mg^{2+} -free phosphate buffered saline. An aliquot (0.5 g) of beads was resuspended in 0.7 ml of α -MEM to make a final volume of 1 ml. For preparation of S cells with internalized beads, 30 μl containing 15 mg of beads were incubated overnight with a confluent cell layer on a 60-mm tissue culture dish ($\sim 6 \times 10^5$ cells/dish) so that the bead-to-cell ratio was $\sim 100:1$. The S cell layer was washed five times with Ca^{2+} - Mg^{2+} -free phosphate-buffered saline to remove any unbound or noninternalized beads. These cells were then trypsinized to remove beads bound on the outside of the cell, neutralized with growth medium, and resuspended in growth medium. Previous studies (22, 23) have demonstrated that this procedure removes all loosely bound but not internalized beads. Internalization of beads was confirmed by electron microscopy and confocal microscopy of calcein/AM-loaded cells (2 μM at 37°C for 30 min). The percentage of phagocytic cells was assessed by flow cytometry as described previously (24), and $69.2 \pm 3.3\%$ of cells ($n = 3$) were found to be phagocytic with this procedure. To assess the relative amount of bead internalization per cell, cells with internalized beads were replated onto 60-mm dishes and incubated for 8 h to allow attachment and spreading. Image analysis measurements were made on the mean projected area of cells occupied by internalized beads ($509 \pm 6.0 \mu\text{m}^2$ /cell with a mean total cell area of $\sim 1200 \mu\text{m}^2$; $\sim 42\%$ coverage).

To test the specificity of cadherin-based mechanotransduction, we used magnetic particles that were coated with anti-N-cadherin antibody or anti-CD-90 antibody (control). BioMag magnetic beads covalently linked to goat anti-mouse IgG (Fc specific) antibody were incubated with mouse anti-human primary antibody (anti-N-cadherin antibody or anti-CD-90 antibody at a concentration of five times Fc binding capacity of IgG beads) in phosphate buffer, pH 8.2, for 1 h at 37°C . These beads were washed three times with PBS, sonicated, and incubated with monolayer of cells for 45 min at 37°C in α -MEM to allow binding to the cell surface. Unbound beads were washed off by PBS.

Force Generation—Force was generated based on electromagnetic attraction of ferric oxide beads as described (25). Briefly, an electromagnet was made from a core of annealed Mu metal (BCL Magnetics, Burlington, Canada). The core was wound with 1600 turns of 16-gauge Belden wire (Electrosonic, Toronto, Canada). A direct current power supply was used that provided adjustable voltage (0–100 V) and current (0–33 A). A magnet pole extension was made so that a consistent distance from the magnet pole to the cell (~ 5 mm) was maintained. A current through the core winding of 20 A produced a flux density of 420 ± 2.5 G with a gradient of 54 G/mm just outside the pole extension. A single 1-s force application was used for all experiments measuring $[\text{Ca}^{2+}]_i$, resulting in a strong force stretching the intercellular junctions between S cells and A cells. In experiments using anti-N-cadherin antibody coated beads, force was applied to the cadherin-mediated attachments.

In some experiments, a ceramic permanent magnet (Gr. 8, $2.2 \times 9.6 \times 11$ cm; Jobmaster, Mississauga, Canada) was used to generate perpendicular forces (26) on S cells (with internalized beads) attached to the dorsal surface of A cells. For these experiments the pole face was parallel with and 1 cm from the cell culture dish surface.

The force generated by magnetic field application to a S cell with internalized beads was estimated using Stokes' law (27) and from direct measurements of the velocities of these cells in fluids of known viscosities as described (25). To maximize applied force, we only selected cells with high bead loading ($>40\%$ of cell volume) and applied a current of 30 A at 60 V to the electromagnet. We reasoned that because S cells are attached to A cells largely through cadherin-mediated adherens junctions (15), the forces applied to the S cells are transferred to these adhesive junctions. Using the above method (25), we estimated that the force applied to these intercellular contacts is 155 ± 18 pN/S-A cell couple.

Cell Viability—Propidium iodide staining was used to determine whether ferric oxide beads and force application cause damage to the cells during the duration of the experiments. Flow cytometry analyses were performed as described (24). Briefly, following internalization of

ferric oxide beads by the cells and force application, the cells were stained with propidium iodide (10 μM ; Calbiochem; 5 min at 37 °C), trypsinized, pelleted, and resuspended in PBS to a cell concentration of $1 \times 10^6/\text{ml}$. The cells were analyzed by flow cytometry.

Microinjection of Fluorescent Actin—The cells for microinjection were subcultured to 50% confluency in 30-mm glass bottom dishes (Willco Wells, Amsterdam, The Netherlands). Needles for microinjection were prepared from glass capillaries (1.5-mm outer diameter; Kwik-fil; World Precision Instruments, Inc., New Haven, CT) and pulled on a micropipette puller (Brown-Flaming; Sutter Instrument Co., San Francisco, CA). For microinjection, the cells were viewed with a Nikon TE-3000 microscope using a 40 \times objective. Microinjections were performed using an Eppendorf micromanipulator model 5171 and transjector model 5246 (Eppendorf, Hamburg, Germany). Rhodamine-labeled nonmuscle monomeric actin (1–2 mg/ml) for injections was prepared in 5 mM Tris-HCl, pH 8.0, 0.2 mM CaCl_2 , and 0.2 mM ATP. All solutions for microinjection were centrifuged for 15 min at 14,000 rpm to remove dust and backloaded. Volumes injected were 5–10% of cell volume.

Statistical Analysis—For continuous variable data, the means and S.E. were computed, and when appropriate comparisons between two groups were made with unpaired Student's *t* tests with the statistical significance set at $p < 0.05$. Analysis of multiple groups was made by ANOVA followed by a post-comparison Scheffe test with the statistical significance set at $p < 0.05$.

RESULTS

Model System for Force Application to Intercellular Junctions—We first developed a model to test whether adherens junctions are mechanotransducers by applying controlled mechanical forces through cells with internalized ferric oxide beads (Fig. 1A). Human fibroblasts were incubated with ferric oxide beads overnight for internalization by phagocytosis (22). Electron microscopy of these cells showed complete internalization of the ferric oxide beads (Fig. 1B). Based on transmitted light microscopy, the optimal amount of bead loading via phagocytosis was determined to be 5 mg/35-mm tissue culture well of confluent cells (~20–30 beads/cell). Notably, higher bead-to-cell ratios did not increase bead loading (Fig. 1C). We estimated the volume of the cell occupied by beads to be $42.4 \pm 5\%$ by confocal microscopy optical sectioning of calcein/AM-loaded cells with internalized beads. This volume was consistent with the estimate obtained by transmitted light microscopy (509 $\mu\text{m}^2/1200 \mu\text{m}^2$; ~42%) described under "Experimental Procedures." The cells with internalized beads were suspended by trypsinization in the presence of calcium to remove surface-bound beads and were then added onto substrate-attached monolayers of fibroblasts. We have previously shown that S cells and A cells rapidly (<15 min) form intercellular adherens junctions (15) that are cadherin-mediated (17).

When an electromagnetic field of 150.3 ± 8.6 Gauss was applied, the S cells were attracted toward the pole of the magnet and moved but were not detached (Fig. 1D), because S cells are attached to A cells through adherens junctions (15). The mechanical force applied to the intercellular junctions was estimated by measuring magnet-induced movement of S cells with internalized beads moving through viscous fluids (see "Experimental Procedures") and was ~150 pN/cell for cells with high bead-loading. When S cells are attached to A cells, this magnetically generated force is applied to the intercellular junctions between the S-A cell couples (Fig. 1, A and D). Following deformation of the S cell when the magnetic force was applied (Fig. 1D), we considered that the resultant increase in membrane tension associated with cellular deformation may activate mechanosensitive channels (e.g. Ca^{2+} -permeable channels; Ref. 28; see below).

To validate our model of intercellular stretching, we tested whether fibroblasts with internalized ferric oxide beads are viable and exhibit normal metabolism with or without force application. At the optimal bead loading of 5 mg/well, these cells exhibited normal morphology and function as shown by

their ability to attach to other cells or to a cell culture substrate. Further, they exhibited similar proportions of proliferating cells as control cultures when analyzed for the percentage of S phase cells by flow cytometry (Fig. 1E). Force application to cells with internalized beads did not cause any detectable plasma membrane damage because their ability to exclude propidium iodide, a membrane impermeant dye, was the same as that of control cells. The mean propidium iodide fluorescence of the group of cells with internalized beads (1.19 ± 0.04 fluorescence channel number), and the group with internalized beads and 4-h force exposure (1.18 ± 0.01) was not statistically different ($p > 0.1$) from control cells (1.10 ± 0.03). An alternative viability assay based on a replating and cell attachment method (29) showed no difference in viability between control and bead-loaded cells ($92.3 \pm 5.4\%$ of control; $p > 0.1$). Immunoblotting of glyceraldehyde-3-phosphate dehydrogenase and the mitochondrial protein COX-1 showed that bead internalization and/or force application did not change the cellular content of these proteins, suggesting that cellular metabolism was unaltered (Fig. 1F).

Mechanical Forces Applied to Intercellular Junctions Induce $[\text{Ca}^{2+}]_i$ Signaling—We investigated whether forces applied to intercellular adherens junctions would activate intracellular calcium signaling. Previous reports on the periodontal fibroblast model used here conclusively demonstrate that intercellular adhesion is dependent on cadherin-mediated adherens junctions (17). After magnetic force application to bead-loaded cells that were attached to substrate-attached A cells, we observed robust $[\text{Ca}^{2+}]_i$ increases in A cells but not in S cells (Fig. 2). The time from force application to maximum $[\text{Ca}^{2+}]_i$ increase varied between 30 and 150 s. We assessed whether movement of beads alone inside the cell would induce a calcium transient by measuring $[\text{Ca}^{2+}]_i$ in substrate-attached cells with internalized beads during magnetic force application. In these cells, no change of $[\text{Ca}^{2+}]_i$ was observed (Fig. 2), indicating that $[\text{Ca}^{2+}]_i$ increases were specific to stretching of intercellular junctions and not due to cytoplasmic disturbance from intracellular bead movement.

We found that the $[\text{Ca}^{2+}]_i$ responses to intercellular stretching decreased as cell-cell contacts matured. Thus, at early stages (15 min) of intercellular attachment, force application visibly displaced (Fig. 1D) magnetite bead loaded suspended cells and induced robust Ca^{2+} transients (65 ± 9.4 nM above base line) in substrate-attached cells (Fig. 3A). This response decreased as intercellular junctions continued to develop under repeated stretching over a time course of 90 min (15 when the applied force of ~150 pN no longer could induce $[\text{Ca}^{2+}]_i$ transients (Fig. 3A). The stretch-induced response appeared to be negatively associated with the intercellular contact area. We measured the area of cadherin and β -catenin staining at the intercellular interface by confocal microscopy and found that intercellular contact area increased over time (Fig. 3B). These time-dependent decreases in Ca^{2+} responses after stretch may reflect a reorganization of intercellular contacts.

Origins of Calcium Transients—We determined the source of Ca^{2+} for the observed rise in $[\text{Ca}^{2+}]_i$. To establish whether the increase of $[\text{Ca}^{2+}]_i$ after force application was due to Ca^{2+} influx or internal mobilization of Ca^{2+} , fura-2-loaded cells were switched to a Ca^{2+} -free buffer containing 2 mM EGTA immediately before force application. Under these conditions, force application failed to induce a defined Ca^{2+} transient ($n = 10$; Fig. 4), indicating that the robust intracellular Ca^{2+} response was dependent at least in part on calcium influx through plasma membrane-permeable channels.

Because a variety of cells express mechanosensitive ion channels (28) that mediate the influx of ions across the plasma

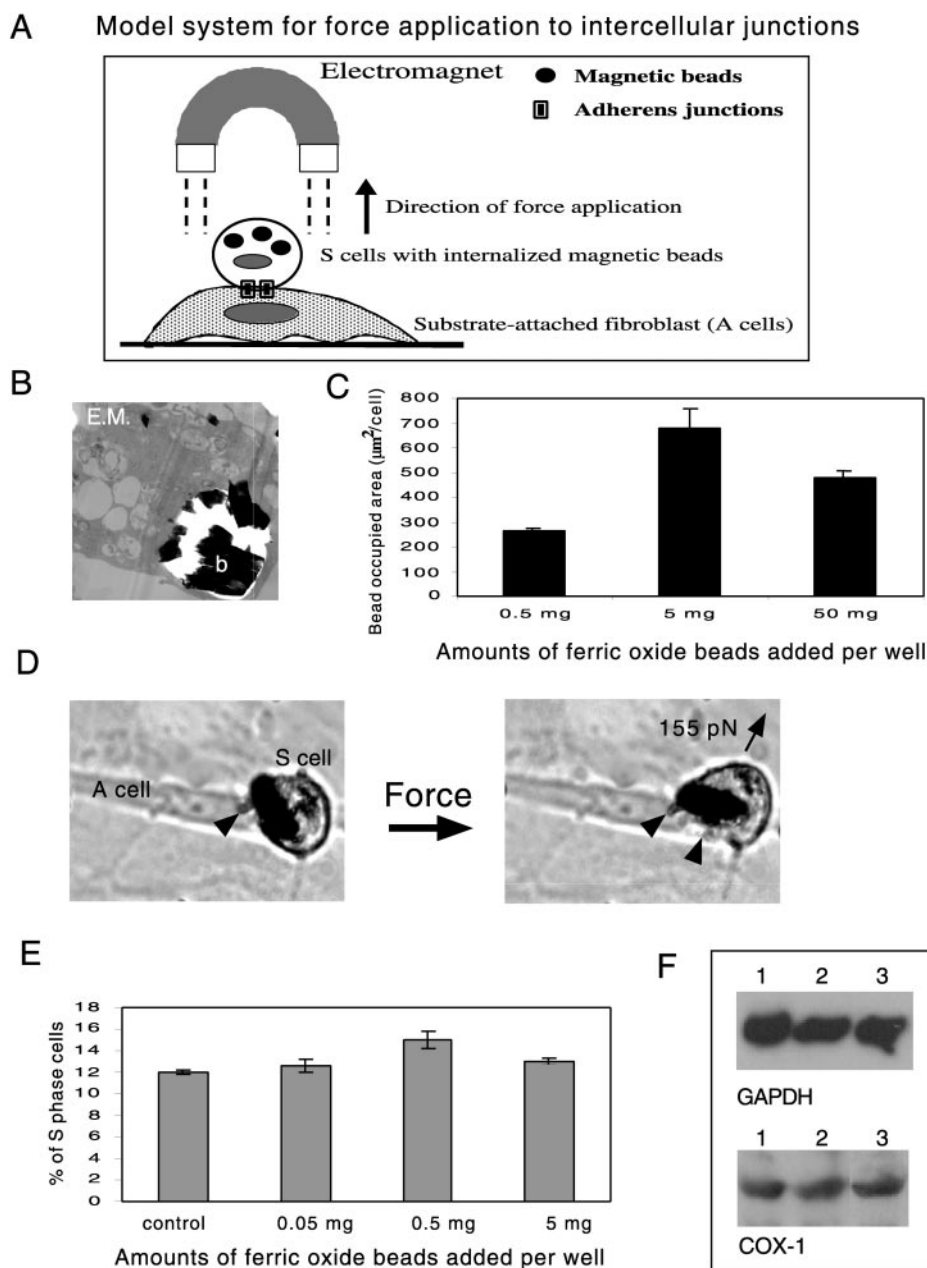


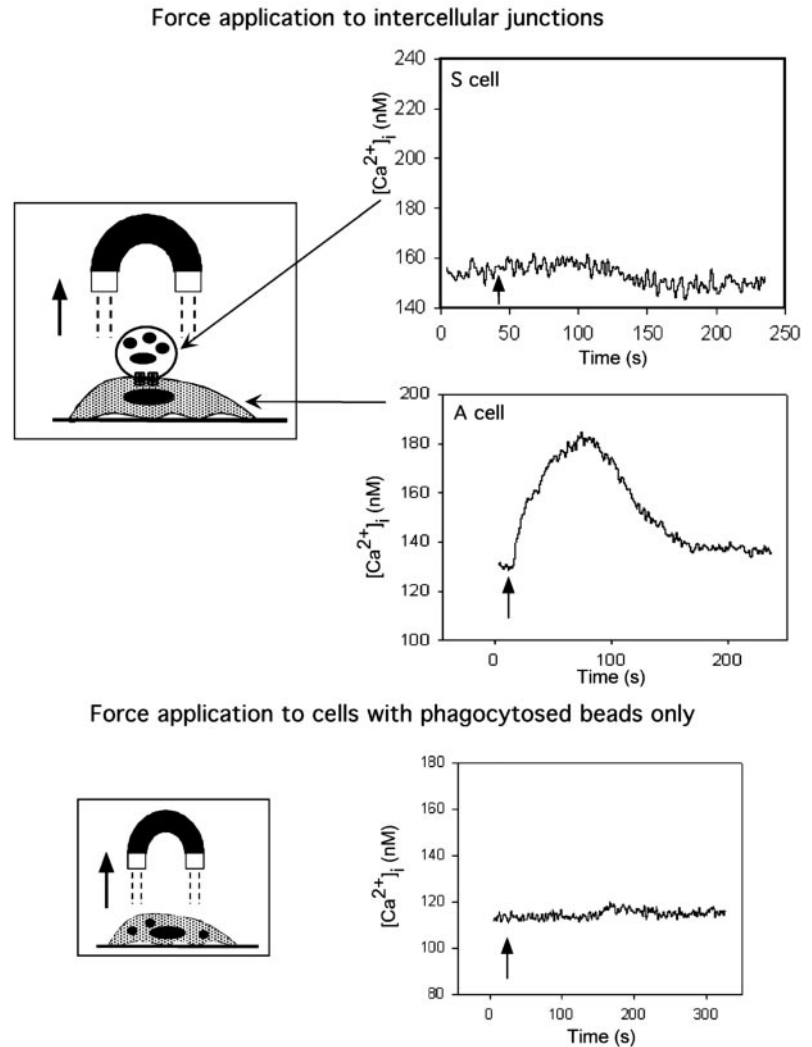
FIG. 1. Model system for applying mechanical forces to intercellular junctions. *A*, schematic diagram of experimental strategy for applying forces to intercellular junctions through electromagnetic attraction of S cells with internalized ferric oxide beads after establishment of intercellular adherens junctions between S and A cells. *B*, electron micrograph (EM) of a suspended fibroblast (S cell) with internalized ferric oxide beads (*b*). Ferric oxide beads were added to a confluent cell monolayer for overnight incubation to ensure high rates of bead internalization. *C*, histograms showing the concentration of ferric oxide beads used for optimal internalization. Various amounts of ferric oxide beads were added onto cell monolayers for overnight incubation. Internalization of beads was confirmed by light microscopy. Unbound beads were washed three times with PBS; cells were trypsinized and replated. The area of cells occupied by internalized beads was quantified to estimate the bead content of the cell (data are the means \pm S.E., $n = 3$). *D*, phase contrast micrographs of S-A cell couples before and during force application. *Left panel*, S cells with internalized ferric oxide beads were co-incubated with A cell layer at 37 °C for 15 min to allow the formation of cell-cell adherens junctions (15) that are cadherin-mediated (17). *Right panel*, under a magnetic field of ~150 Gauss (direction indicated by arrow), S cells with high magnetite content move toward the magnet and the intercellular junctions between the S and A cells are stretched (~155 pN/cell). *E*, proliferative capacity of cells with internalized beads was examined in cells that were trypsinized, fixed, permeabilized, and stained with 4',6-diamidino-2-phenylindole, HCl. The percentage of S phase cells was estimated by flow cytometry. Note that the percentage of S phase cells in the group with internalized beads is not statistically different than the control group (data are the means \pm S.E., $n = 3$). *F*, to examine possible metabolic disturbances by internalization of large amounts of ferric oxide particles, the cells were lysed, and the lysates were immunoblotted using antibodies against glyceraldehyde-3-phosphate dehydrogenase and the mitochondrial protein COX-1. *Lane 1*, attached control cells; *lane 2*, attached cells with internalized beads; *lane 3*, cells with internalized beads exposed to 4 h of constant force. Note that protein content was not changed by bead internalization or force applications to cells.

membrane in response to stretching, we examined whether mechanosensitive channels play a role in intercellular stretch-induced $[\text{Ca}^{2+}]_i$ responses. We performed the stretching experiments in the presence of 1 mM GdCl_3 , an agent that blocks mechanosensitive channels in oocytes (30) and in periodontal fibroblasts (25). None of the cells treated with GdCl_3 responded

to intercellular stretching ($n = 8$; Fig. 4), indicating that mechanosensitive channels may play an important role in mediating the stretch response.

Activation of mechanosensitive ion channels allows MnCl_2 to permeate cells and quench fura-2 (31). In the presence of 1 mM MnCl_2 we observed a steep drop in fluorescence after applica-

FIG. 2. Application of physical forces to intercellular junctions induces Ca^{2+} transients. A robust Ca^{2+} response (65.0 ± 9.4 nM above base line; $n = 15$) was induced immediately after force application (arrow) in A cells but not in S cells ($n = 8$). Well spread, A cells with internalized beads showed no visible signs of displacement when the same magnetic field was applied. No Ca^{2+} response was observed ($n = 10$) in these cells, indicating that the Ca^{2+} transient is caused by the stretching of the cell-cell junctions but not by movement of beads inside the cell.



tion of magnetic force caused by influx of Mn^{2+} and quenching of fura-2 fluorescence when measured at the isosbestic point (356 nm; Fig. 4). In the absence of MnCl_2 , there was no significant change in fura-2 fluorescence intensity ($n = 10$; Fig. 4, middle left panel inset), indicating that there was no dye loss because of membrane damage. Collectively, these results indicate that stretching cells at intercellular junctions induces Ca^{2+} transients as a result of calcium entry through mechanosensitive ion channels.

To test whether Ca^{2+} is released from ER stores in response to stretching of intercellular junctions, the cells were loaded with mag-fura-2 (18). Examination of these cells showed that the dye was compartmentalized in discrete vesicles, consistent with localization to the ER stores. Force applied to the intercellular junctions produced no change in the mag-fura-2 ratio (Fig. 4). Addition of ATP to these cells induced a sharp reduction of the mag-fura-2 ratio followed by a rapid recovery to base line (Fig. 4, middle right panel inset) because of calcium efflux from ER stores, indicating the ER stores in these cells are functional (19). These data suggested that the $[\text{Ca}^{2+}]_i$ increase in response to stretching is due to calcium influx, possibly through mechanosensitive ion channels but is not dependent on internal mobilization of calcium.

Intercellular mechanotransduction via calcium wave propagation through gap junctions has been shown in airway epithelial cells (9, 10) and in osteoblastic cells (11). We investigated the possibility that the intercellular stretch-induced $[\text{Ca}^{2+}]_i$ response could be due to transfer of second messengers from

the S cells to A cells through gap junctions and not due to the stretching of adherens junctions. We stretched S-A cell couples in the presence of inhibitors of gap junctional communication including β -glycyrrhetic acid (32, 33) and the connexin43 mimetic peptide GAP 27 (amino acid sequence SRPTEKTIFII). Both of these agents have been shown to be potent inhibitors of gap junction-mediated dye transfer in human fibroblasts (15). β -Glycyrrhetic acid, a saponin that causes gap junction disassembly and connexin43 dephosphorylation (34), did not affect the intercellular stretch-induced $[\text{Ca}^{2+}]_i$ response (71 ± 13.1 nM above base line, $p > 0.2$ compared with controls; $n = 7$; Fig. 4). Specific blockade of gap junctional communication was achieved by incubation with GAP 27, which has the same amino acid sequence as a part of the extracellular loop of connexin43, the most prominent gap junction protein in human gingival fibroblasts (15). This peptide acts by perturbing connexin-connexin interactions and channel integrity (35, 36) but did not inhibit intercellular stretch-induced $[\text{Ca}^{2+}]_i$ response to any significant extent (73 ± 12.5 nM above base line, $p > 0.2$ compared with controls; $n = 5$, Fig. 4). These results suggest that gap junctions are not involved in the generation of intercellular stretch-induced $[\text{Ca}^{2+}]_i$ response.

Cadherins as Intercellular Mechanotransducers—We characterized the specific adhesive receptors for intercellular stretch-induced activation of mechanosensitive ion channels. In human fibroblasts, confluent but not sparse cultures expressed abundant surface N-cadherin as detected by flow cytometry (Fig. 5, A–C), indicating that expression of cell surface N-cadherin is

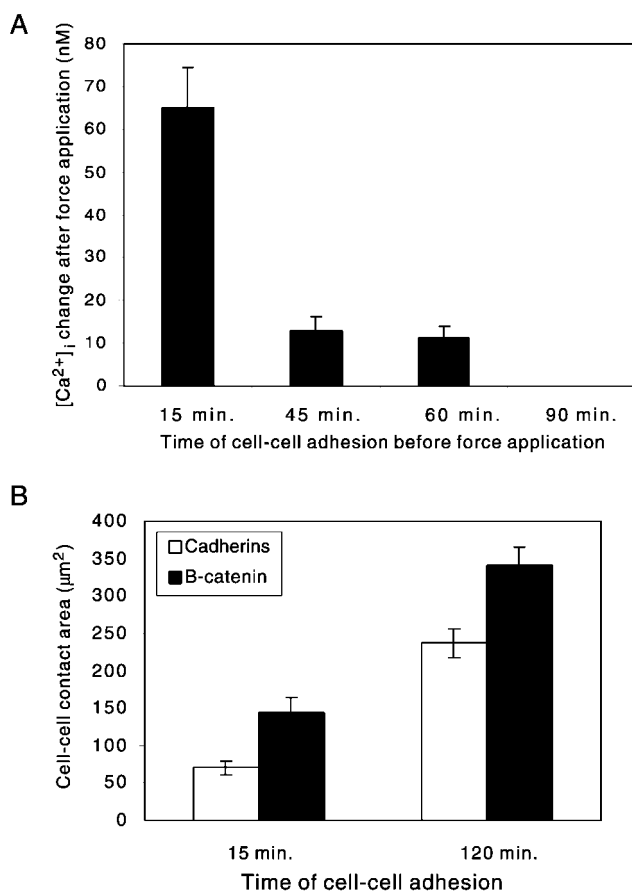


FIG. 3. Maturation of intercellular junctions inhibits force-induced calcium responses. **A**, the amplitude of intracellular calcium transients was measured at various times after incubation of S cells on A cell monolayers. After 15 min of cell-cell contact, $[Ca^{2+}]_i$ was increased within seconds after force application at the cell-cell junction. After 90 min of cell-cell adhesion, no $[Ca^{2+}]_i$ response was induced by force. **B**, temporal increase of cell-cell contact area as measured by confocal sections of cell-cell junctions (17) stained for cadherins and β -catenins. The data are the means \pm S.E. ($n = 3$ independent experiments) of fluorescence area imaged by optical sections obtained at the level of intercellular junctions.

regulated by the extent of intercellular contact. The cells were incubated with N-cadherin antibody-coated Biomag beads and subjected to stretching. Previous studies have shown that anti-cadherin antibody-coated beads attach specifically to N-cadherin expressing cells through adherens junctions-like structures (37). When magnetic force was applied to N-cadherin-coated Biomag beads that were attached to the surface of confluent human fibroblasts, we observed robust $[Ca^{2+}]_i$ transients similar to that obtained from stretching intercellular junctions (Fig. 5G; time from force application to peak = 120 s). Application of magnetic fields to cells preincubated with anti-mouse Fc antibody-coated beads failed to produce any detectable $[Ca^{2+}]_i$ responses (Fig. 5E) because there was only very limited bead attachment. Further, we were not able to obtain Ca^{2+} responses from cells in sparse cultures (Fig. 5F), probably because N-cadherin expression on the cell surface was not sufficient for the attachment of beads (Fig. 5B, inset). Because these cellular responses to beads could be due to stretching of the cell membrane independent of cadherins, we prepared beads coated with an antibody to the glycosyl phosphatidylinositol-linked protein CD90, which does not associate with cortical actin filaments. The gingival fibroblasts expressed abundant cell surface CD90, and beads coated with antibody to CD90 attached strongly to the cells (Fig. 5D). However, CD90 antibody-coated beads elicited no calcium response after force

application (Fig. 5H). Collectively, these data indicate that the stretching response was in part cadherin-mediated and was not due simply to membrane stretching independent of actin engagement.

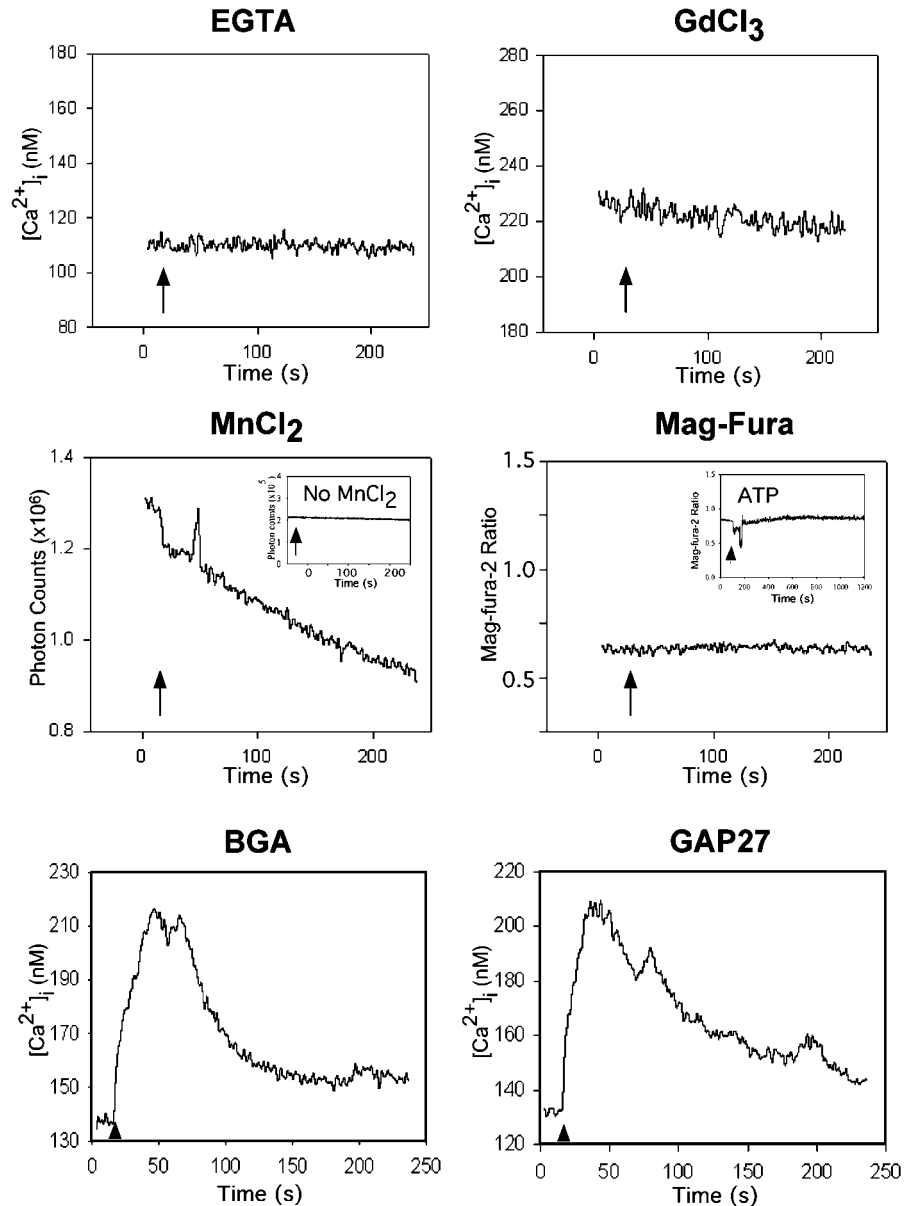
Force-induced Actin Assembly at Intercellular Contacts Is Calcium-dependent—Because $[Ca^{2+}]_i$ regulates the assembly and turnover of actin filaments (38), which in turn are major components of intercellular junctions, we examined the possibility that $[Ca^{2+}]_i$ transients generated from stretching intercellular junctions regulate actin polymerization. We stretched S-A cell couples in which A cells were microinjected with rhodamine-labeled monomeric actin. The microinjected rhodamine-labeled actin monomers were fully functional as shown by their incorporation into stress fibers after incubation with serum at 37 °C for 45 min (Fig. 6A). When continuous force was applied to S cells and intercellular junctions were stretched for 10 min, we observed actin assembly at sites of intercellular contacts (Fig. 6B). This force-induced rearrangement of actin is consistent with previous studies showing that actin stress fibers elongate in response to contractile stress transmitted through adherens junctions in fibroblasts (8). To quantify the amount of whole cell polymerized actin, we immunoblotted the Triton-insoluble fraction of S cell-A cell couples with established intercellular junctions (after 3 h of cell-cell contacts) (17) with or without force application and probing against β -actin, β -catenin, and cadherins (Fig. 6C). We found that force application (4 h) significantly increased polymerized β -actin by 72.5% as measured by densitometry of immunoblots (17.6 ± 2.9 units; control, 10.2 ± 1.6 units; $n = 3$, $p < 0.05$), whereas the recruitment of β -catenin and cadherins to the cytoskeletal fraction was unaltered (Fig. 6C). To test whether this force-induced actin rearrangement was dependent on $[Ca^{2+}]_i$, we buffered intracellular calcium transients by treating the S-A cell couples with $10 \mu M$ BAPTA/AM prior to stretching (Fig. 6B). Under these conditions, force application did not produce any visible changes in staining for actin filaments, suggesting that increased $[Ca^{2+}]_i$ is required for force-induced actin rearrangement.

DISCUSSION

The Model System—To study how mechanical signals are transmitted from cell to cell and how multicellular adaptive responses to mechanical forces are coordinated, we have developed a novel model system in which magnetic forces are applied to intercellular junctions in cells containing internalized magnetite beads. Although intercellular junctions are widely studied in endothelial and epidermal cells, there have been few studies in fibroblasts. We used periodontal fibroblasts in our model because they form only one type of cell-cell adhesive contact (adherens junctions) that are largely cadherin-mediated (17). In contrast, intercellular junctions in epithelial cells involve several distinct structures such as tight junctions, adherens junctions, and desmosomes that complicate the interpretation of intercellular mechanotransduction. Our system therefore allows the delivery of direct and specific stretching forces to the intercellular adherens junctions of fibroblasts.

The development of a novel approach was required to overcome limitations of currently used methods that apply forces to confluent cell layers using either fluid flow chambers or stretching of flexible substrata that inevitably involve activation of both cell-substrate and cell-cell adhesion complexes. Our model has several advantages. First, the model applies forces directly to intercellular adherens junctions. Second, fibroblasts exhibit high rates of phagocytosis (23) of various particles including ferric oxide beads. Therefore, it has been possible to load high levels of magnetite into cells and thereby generate sufficiently high forces to study calcium transients. Third, in the flexible membrane stretching system, it is difficult, if not

FIG. 4. Ca^{2+} influx induced by stretching intercellular junctions is mediated by mechanosensitive ion channels and is not dependent on gap junctions. *Top panels,* Ca^{2+} responses to force application are abolished in the presence of EGTA or GdCl_3 , indicating Ca^{2+} influx through mechanosensitive channels is required. *Middle left panel,* stretching (arrow) through intercellular junctions caused MnCl_2 quenching of fura-2 fluorescence when measured at the isobestic point (356 nm) during stretching, further suggesting increased permeability of stretch-activated channels. *Inset,* note the absence of fluorescence change, indicating that there was no leakage of fura-2. *Middle right panel,* the increase in $[\text{Ca}^{2+}]_i$ is not dependent on release from ER stores as mag-fura-2 reported no changes after force application. ATP-induced ER store release of Ca^{2+} is included as a positive control for activation of ER stores (*inset*). *Bottom panels,* the robust Ca^{2+} response to force application is not inhibited by $20 \mu\text{M}$ β -glycyrrhetic acid (*BGA*) or the gap junction mimetic peptide (*GAP27*), indicating that gap junctions are not required.



impossible, to quantify the forces applied to intercellular junctions because the strain but not the stress is measured. In contrast, we were able to estimate the magnitude of forces applied to the intercellular junctions by measuring the movements of cells with internalized beads in viscous fluids. Further, the magnitude of applied forces can be controlled by varying the strength of the magnetic field.

Using this system, we were able to apply forces of ~ 50 – 155 pN/cell or ~ 10 – 30 dynes/cm² to intercellular adhesive contacts. Evidently, intercellular contacts are able to withstand these forces without separation because the S-A cell couples remained attached despite continuous application of forces (>30 min). Shear stress studies on endothelial cells have used forces from 20 to 150 dynes/cm² with no significant detachment of cells from the substrates at >150 dynes/cm² (39). Similar force levels were used in cadherin-mediated cell-cell contacts in which E-cadherin positive breast tumor cell aggregates could not be disaggregated when exposed to shear forces in excess of >100 dynes/cm² (40). The forces we applied (3 pN/ μm^2 of cell area) are also similar in magnitude to forces generated by the cell; rearward traction forces on the dorsal surface of migrating fibroblasts are estimated to be 1 pN/ μm^2 (41). We have also

demonstrated that bead loading and subsequent stretching of these cells did not damage the cell membranes at force levels of ~ 155 pN/cell and that stretched cells exhibit normal metabolism as measured by immunoblotting of glyceraldehyde-3-phosphate dehydrogenase and the mitochondrial protein COX-1.

Stretch Activation of Mechanosensitive Channels through Cadherins—We have found that when force is applied to intercellular junctions, there was marked twisting of S cells on A cells. We have shown previously that the attachments between S cells and A cells are largely cadherin-mediated (17). Our current data illustrate that stretching forces applied through these adhesive contacts induce rapid calcium transients that return to base line within 4 min. Notably, A cells but not S cells exhibited calcium responses to stretching at intercellular junctions. Because S cells are rounded and A cells are well spread, these findings are consistent with previous results showing that cell shape is critical in determinant of fibroblast responses to substrate stretch (42). The lack of stretch-induced calcium signal in the S cells was not due to fluorescence quenching of fura-2 by the internalized magnetite because we were able to obtain reproducible and stable base-line signals to estimate calcium concentration. We suggest that the lack of response in

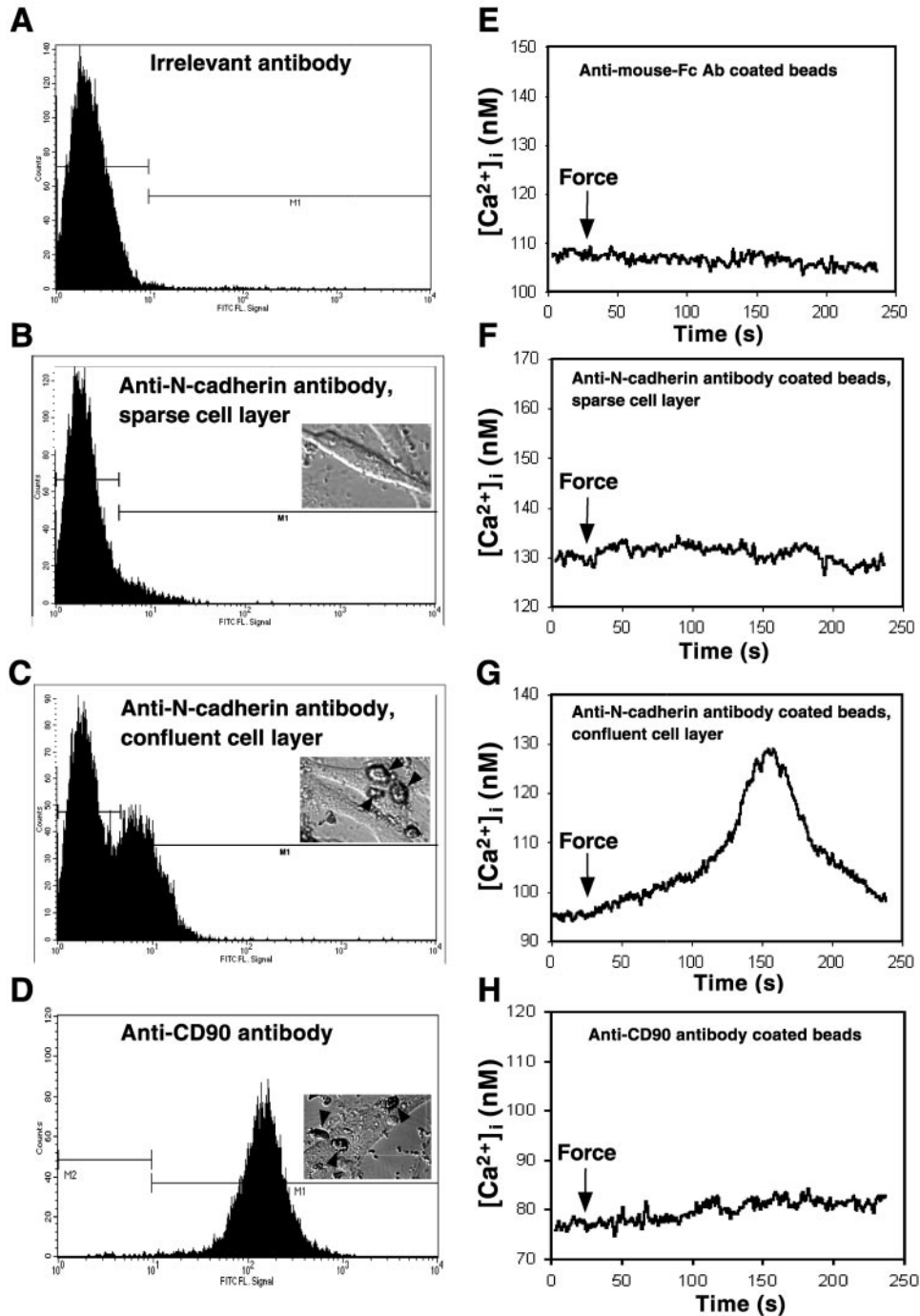


FIG. 5. Force applied through N-cadherin induces Ca^{2+} transients. A–C, human fibroblasts express N-cadherin on the cell surface in confluent cultures but not in sparse cultures. Flow cytograms of unpermeabilized cells show positive staining of N-cadherin using an anti-N-cadherin antibody against the extracellular domain of N-cadherin (Clone GC-4) followed by FITC goat anti-mouse monoclonal antibody (C). Vital immunofluorescent staining was performed on cells in suspension in the presence of Ca^{2+} . Note that a significant percentage of confluent cells (C) but not sparse cells (B) are positive for N-cadherin (>35%) compared with cells stained with FITC-goat anti-mouse antibody only (A, secondary antibody). Differential interference contrast images showed significant binding of anti-N-cadherin antibody-coated magnetic beads (arrowheads) to confluent cell layer (C, inset) but not in sparse cell layer (B, inset). Human fibroblasts express abundant CD90 on their surface as shown in flow cytograms of unpermeabilized cells (D). The cells incubated with anti-CD90 antibody-coated magnetic beads showed significant bead binding (D, inset, arrowheads). Electromagnetic force applied to anti-mouse Fc antibody-coated magnetic beads induces no Ca^{2+} response (E, $n = 8$). The same amount of force applied to anti-N-cadherin antibody-coated beads incubated with N-cadherin-expressing confluent cells (C) induced a Ca^{2+} transient (G; $n = 7$). No Ca^{2+} transients were seen in sparse cells (F, $n = 8$) nor in cells with anti-CD90 antibody-coated beads (H, $n = 8$), suggesting that this is indeed a cadherin-mediated response.

the S cells is due to the relative paucity of cortical actin filaments in these rounded cells and their consequent inability to transmit forces from the cadherin-mediated intercellular junctions to mechanosensitive channels.

The $[\text{Ca}^{2+}]_i$ response was eliminated when cells were incubated in calcium-free buffer with EGTA or in the presence of

the putative stretch-activated channel inhibitor gadolinium chloride (30), suggesting that calcium influx through stretch-activated channels is the origin of the $[\text{Ca}^{2+}]_i$ response. Increased conductance of ion channels after stretching is further supported by quenching of fura-2 fluorescence in the presence of MnCl_2 . We suggest that forces transmitted through adher-

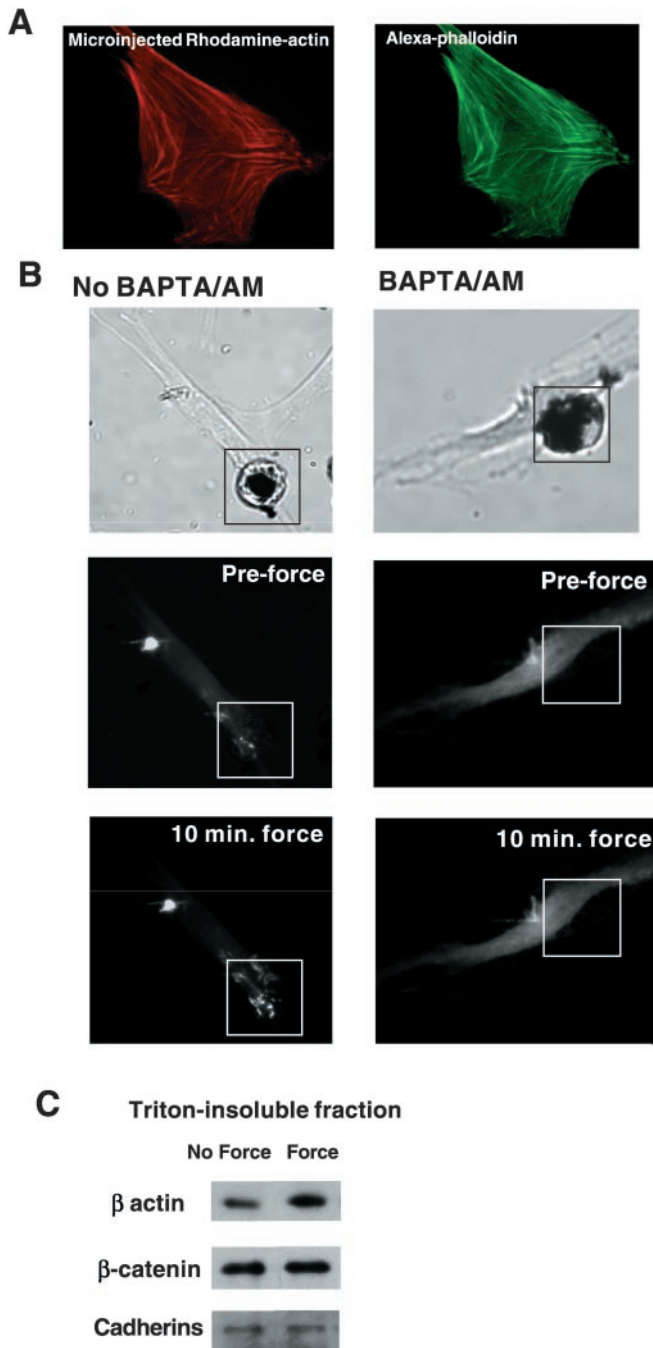


FIG. 6. Intercellular force application induces localized actin assembly. *A*, micrographs of a human fibroblast with microinjected rhodamine-labeled actin monomers (red) that have become incorporated into stress fibers stained with Alexa-phalloidin (green). The cells were microinjected with 2 mg/ml (~5–10% of cell volume) rhodamine-labeled monomeric actin, incubated at 37 °C for 30 min, followed by fixation and staining with Alexa Fluor 488 phalloidin. Note the incorporation of injected rhodamine-actin into stress fibers, indicating that the rhodamine-actin monomers are functional. *B* and *C*, force application to cell-cell junctions induces rearrangement of actin. Phase contrast and fluorescence micrographs of substrate-attached fibroblast in contact with a suspended cell loaded with ferric oxide beads with or without 10 μ M BAPTA/AM treatment (*B*). The attached cell was injected with rhodamine-labeled monomeric actin before force application. Note the increase in fluorescence of rhodamine-actin at the cell-cell contact site after force application for 10 min (*box*). This force-induced accumulation of actin at the cell-cell contacts was abolished by intracellular buffering of Ca^{2+} using BAPTA/AM treatment. Immunoblotting of the Triton-insoluble fraction of the cell-cell couples after force application for 4 h using anti- β -actin, β -catenin, and pan-cadherins antibodies showing increased assembly of β -actin into filaments after force application at cell-cell junctions (*C*).

ens junctions cause changes in membrane tension, thereby leading to alteration of the open probability of mechanosensitive channels (28) and perhaps the activation of other signaling pathways.

Because mechanical signals may be transduced through specific transmembrane receptors (43), we hypothesized that activation of stretch-activated channels during intercellular stretching is mediated through adherens junctions. Forces applied through substrate attachments via integrins can activate mechanosensitive ion channels (25). Here we have demonstrated that forces applied to cadherin-mediated adherens junctions via anti-N-cadherin antibody-coated beads (37) can induce similar $[Ca^{2+}]_i$ responses as shown by stretching of the S cell-A cell couples. Consistent with this notion, we found that the $[Ca^{2+}]_i$ response amplitude was positively related to the amount of N-cadherin expressed on the cell surface, suggesting that a critical level of cadherin-binding is required for this type of mechanotransduction. However, we cannot rule out contributions by other intercellular adhesion molecules possibly including integrins.

In stretching experiments using beads coated with antibody to the glycosyl phosphatidyl-inositol-linked protein CD90, we found limited generation of calcium transients. These results suggest that cadherin-mediated adherens junctions are intercellular mechanotransducers capable of increasing the permeability of stretch-activated channels and that cadherin linkages to subcortical actin may be important. Indeed a notable finding was that over time, the amplitude of calcium transients decline as the surface area of intercellular cadherin staining increases. This suggests that the calcium transients that are mediated by cell-cell stretching are related to the force generated by magnetic field (a constant in all experiments) and the surface area of cadherin-mediated intercellular contact. We propose that as more cadherin-mediated junctions are being formed (as indicated by increased cell-cell cadherin staining) during the time of contact, the force applied to each cadherin-mediated junction decreases as the strain is distributed over an increased surface area, resulting in reduced calcium responses.

We considered that the $[Ca^{2+}]_i$ responses could have been mediated through gap junctions (9–11) because periodontal fibroblasts can form extensive gap junctions *in vitro* (15). We found that A cells but not S cells exhibited calcium transients in response to stretch, suggesting that intercellular flow of second messenger molecules through gap junctions from S to A cells was not involved. Further, treatment of cells with various inhibitors of gap junctions, such as β -glycyrrhetic acid and GAP 27 peptides, did not alter the $[Ca^{2+}]_i$ response in A cells, indicating that gap junctional communication is not required for this type of stretch response.

Coordination of Multicellular Responses to Mechanical Forces Involves Actin—We have shown previously the importance of actin in the formation and maintenance of intercellular junctions in fibroblasts (17), and in this study we demonstrated that actin filament assembly is regulated by cadherin-mediated mechanotransduction processes. In cells microinjected with rhodamine-labeled actin monomers, stretching of intercellular junctions induced accumulation of actin filaments adjacent to force application sites. This finding is consistent with observations in contracting embryonic wounds in which actin cables (intracellular actin filaments linked to neighboring cells via cell-cell junctions) coordinate wound closure (44). It has been suggested that the primary stimulus for actin reorganization at the wound edge is a change in the pattern of stresses in the epidermis rather than a ligand/receptor-mediated signal (44). This contention is further supported by the observation that tumor growth factor- β 1, which can facilitate contraction

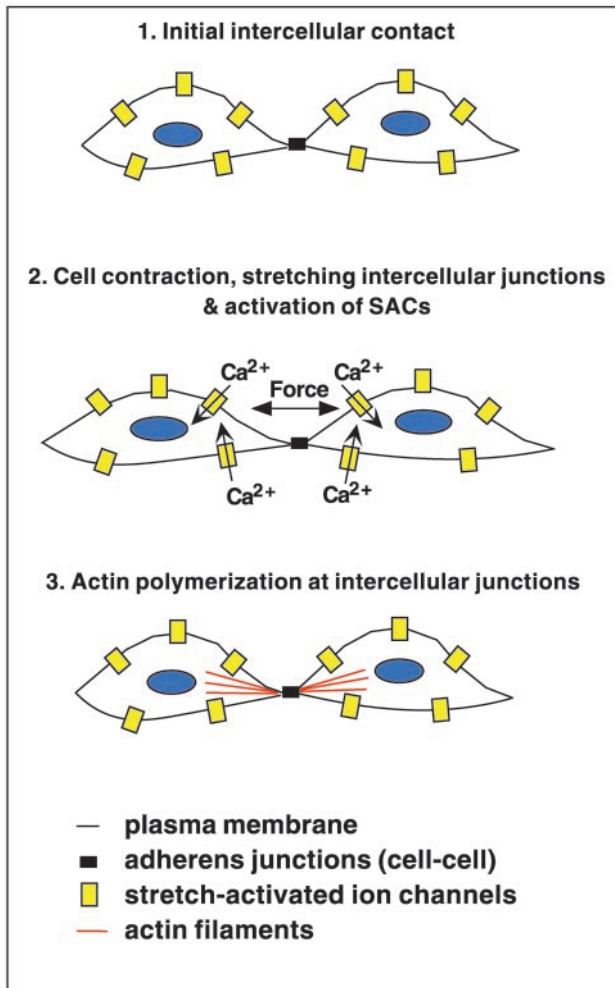


FIG. 7. Intercellular adherens junctions mediate mechanotransduction. A proposed scheme for intercellular mechanical signaling and how force regulates the reinforcement of adherens junctions in fibroblasts. Adjacent fibroblasts form intercellular contacts through cadherin-mediated adherens junctions (*step 1*). As adjacent cells contract and apply tractional forces to each other through adherens junctions, stretch-activated ion channels are opened, allowing influx of Ca^{2+} (*step 2*). This process results in actin recruitment at the intercellular junctions (*step 3*). Accumulation of actin filaments at intercellular contacts following stretching may mechanically reinforce these junctions and dampen subsequent, force-induced opening of stretch-activated channels (see Fig. 3A for data in support of this notion).

and force generation in healing wounds, induces the rearrangement of adherens junctions as a result of actin cytoskeletal reorganization (45). In our model system, the stretch-induced accumulation of actin was abolished by intracellular buffering of calcium with BAPTA/AM, indicating that actin reorganization is mediated through the intracellular calcium signals initiated by stretch-activated channel activation when the intercellular junctions are stretched.

Mechanical Force Regulates the Strengthening of Intercellular Contacts—In addition to cell-cell attachment (1), we suggest that cadherin-mediated adherens junctions also play a role in mechanotransduction in multicellular syncytia. Adherens junctions are biologically important in coordination of wound closure in connective tissue cells *in vivo* (2), and previous studies have shown that maintenance of fibroblastic intercellular contacts depends on the contractility of the actin cytoskeleton (6). However, it is uncertain how intercellular mechanical forces stabilize these contacts. Based on the data presented here, we propose a model of intercellular mechanotransduction (Fig. 7). First, actin-myosin-derived contractile forces transmitted

through intercellular adherens junctions mediate activation of stretch-activated ion channels in neighboring cells, a process that is analogous to the activation of calcium-permeable channels observed in migrating fish keratocytes (46). Second, calcium transients initiate actin filament assembly (47), a process that is particularly enhanced at sites immediately adjacent to intercellular contacts. Third, because actin assembly induced by force increases membrane rigidity (48), actin filament assemblies adjacent to adherens junctions stabilize intercellular contacts and reinforce the membrane cortex. This reinforcement serves to dissipate localized membrane tension, and consequently, the conductance of stretch-activated ion channels returns to basal levels. Indeed, cells become refractory to force-induced opening of stretch-activated channels after prolonged intercellular contact (Fig. 3A).

In conclusion, on the basis of our data and the proposed model, we suggest that connective tissue cells can coordinate their responses to mechanical forces through adherens junctions. These junctions mediate the activation of stretch-activated ion channels and subsequently facilitate the reorganization of actin filaments.

Acknowledgments—We thank Cheung Lo for assistance with cell cultures, Austin Chen for assistance with immunoblotting, Lowell Langille and Gregory Downey for advice, Wilson Lee for assistance with flow cytometry, and Paul Janmey, András Kapus, Mingyao Liu, and Shao-Ying Hua for helpful comments on the manuscript.

REFERENCES

1. Takeichi, M. (1995) *Curr. Opin. Cell Biol.* **7**, 619–627
2. Gabbiani, G., and Rungger-Brandle, E. (1981) *Tissue Repair and Regeneration: Handbook of Inflammation* (Glynn, L. E., ed) Vol. 3, pp. 1–50, Elsevier Science Publishers B.V., Amsterdam
3. Xu, J., Liu, M., Tanswell, A. K., and Post, M. (1998) *Am. J. Physiol.* **275**, L545–L550
4. Wang, X., and Gerdes, A. M. (1999) *J. Mol. Cell. Cardiol.* **31**, 333–343
5. Adams, C. L., and Nelson, W. J. (1998) *Curr. Opin. Cell Biol.* **10**, 572–577
6. Glogoukova, N. A., Krendel, M. F., Alieva, N. O., Bonder, E. M., Feder, H. H., Vasiliev, J. M., and Gelfand, I. M. (1998) *Proc. Natl. Acad. Sci. U. S. A.* **95**, 4362–4367
7. Danjo, Y., and Gipson, I. K. (1998) *J. Cell Sci.* **111**, 3323–3332
8. Ragsdale, G. K., Phelps, J., and Luby-Phelps, K. (1997) *Biophys. J.* **73**, 2798–2808
9. Boitano, S., Sanderson, M. J., and Dirksen, E. R. (1994) *J. Cell Sci.* **107**, 3037–3044
10. Hansen, M., Boitano, S., Dirksen, E. R., and Sanderson, M. J. (1996) *J. Cell Sci.* **108**, 2583–2590
11. Xia, S. L., and Ferrier, J. (1992) *Biochem. Biophys. Res. Commun.* **186**, 1212–1219
12. Noria, S., Cowan, D. B., Gotlieb, A. I., and Langille, B. L. (1999) *Circ. Res.* **85**, 504–514
13. Beertsen, W., and Everts, V. (1980) *J. Periodont. Res.* **16**, 524–541
14. Shore, R. C., Berkovitz, B. K. B., and Moxham, B. (1981) *J. Anat.* **133**, 67–76
15. Ko, K., Arora, P., Lee, W., and McCulloch, C. (2000) *Am. J. Physiol.* **279**, C147–C157
16. Pender, N., and McCulloch, C. A. (1991) *J. Cell Sci.* **100**, 187–193
17. Ko, K., Arora, P., Bhide, V., Chen, A., and McCulloch, C. (2001) *J. Cell Sci.* **114**, 1155–1167
18. Hofer, A. M., Landolfi, B., Debellis, L., Pozzan, T., and Curci, S. (1998) *EMBO J.* **17**, 1986–1995
19. Golovina, V. A., and Blaustein, M. P. (1997) *Science* **275**, 1643–1648
20. Grynkiewicz, G., Poenie, M., and Tsien, R. Y. (1985) *J. Biol. Chem.* **260**, 3440–3450
21. Ko, K., Glogauer, M., McCulloch, C. A., and Ellen, R. P. (1998) *Infect. Immun.* **66**, 703–709
22. McKeown, M., Knowles, G., McCulloch, C. A. (1990) *Cell Tissue Res.* **262**, 523–530
23. Knowles, G. C., McKeown, M., Sodek, J., and McCulloch, C. A. (1991) *J. Cell Sci.* **98**, 551–558
24. Lee, W., Sodek, J., and McCulloch, C. A. (1996) *J. Cell. Physiol.* **168**, 695–704
25. Glogauer, M., and Ferrier, J., and McCulloch, C. A. (1995) *Am. J. Physiol.* **269**, C1093–C1104
26. Glogauer, M., and Ferrier, J. (1998) *Pfluegers Arch. Eur. J. Physiol.* **435**, 320–327
27. Massey, B. S. (1968) *Mechanics of Fluids* pp. 154–155, Van Nostrand Co., Princeton, NJ
28. Sackin, H. (1995) *Annu. Rev. Physiol.* **57**, 333–353
29. Kulkarni, G. V., and McCulloch, C. A. (1994) *J. Cell Sci.* **107**, 1169–1179
30. Yang, X. C., and Sachs, F. (1989) *Science* **243**, 1068–1071
31. Kirber, M. T., Walsh, J. V., and Singer, J. J. (1988) *Pfluegers Arch. Eur. J. Physiol.* **412**, 339–345
32. Davidson, J. S., Baumgarten, I. M., and E. H. Harley. (1986) *Biochem. Biophys. Res. Commun.* **134**, 29–36

33. Spanakis, S. G., Petridou, S., and Masur, S. K. (1998) *Invest. Ophthalmol. Vis. Sci.* **39**, 1320–1328
34. Guan, X., Wilson, S., Schlender, K. K., and Ruch, R. J. (1996) *Mol. Carcinog.* **16**, 157–164
35. Chaytor, A. T., Evans, W. H., and Griffith, T. M. (1997) *J. Physiol.* **503**, 109–119
36. Dora, K. A., Martin, P. E. M., Chaytor, A. T., Evans, W. H., Garland, C. J., and Griffith, T. M. (1999) *Biochem. Biophys. Res. Commun.* **254**, 27–31
37. Levenberg, S., Katz, B. Z., Yamada, K. M., and Geiger, B. (1998) *J. Cell Sci.* **111**, 347–357
38. Janmey, P. A. (1994) *Annu. Rev. Physiol.* **56**, 169–191
39. Girard, P. R., Helmlinger, G., and Nerem, R. M. (1993) *Physical Forces and the Mammalian Cell* (Frangos, J., ed) pp. 193–222, Academic Press, New York
40. Byers, S. W., Sommers, C. L., Hoxter, B., Mercurio, A. M., and Tozeren, A. (1995) *J. Cell Sci.* **108**, 2053–2064
41. Galbraith, C. G., and Sheetz, M. P. (1997) *Proc. Natl. Acad. Sci. U. S. A.* **94**, 9114–9118
42. Arora, P. D., Bibby, K. J., McCulloch, C. A. (1994) *J. Cell. Physiol.* **161**, 187–200
43. Meyer, C. J., Alenghat, F. J., Rim, P., Fong, J. H., Fabry, B., and Ingber, D. E. (2000) *Nat. Cell Biol.* **2**, 666–668
44. Brock, J., Midwinter, K., Lewis, J., and Martin, P. (1996) *J. Cell Biol.* **135**, 1097–1107
45. Hurst, V. IV, Goldberg, P. L., Minnear, F. L., Heimark, R. L., and Vincent, P. A. (1999) *Am. J. Physiol.* **27**, L582–L595
46. Lee, J., Ishihara, A., Oxford, G., Johnson, B., and Jacobson, K. (1999) *Nature* **400**, 382–386
47. Janmey, P. A. (1998) *Physiol. Rev.* **78**, 763–781
48. Glogauer, M., Arora, P., Yao, G., Sokholov, I., Ferrier, J., and McCulloch, C. A. G. (1997) *J. Cell Sci.* **110**, 11–21